Possible alternative parity bands in the heaviest nuclei

T. M. Shneidman,[1] G. G. Adamian,[1,2] N. V. Antonenko,[1,3] and R. V. Jolos[1]
[1]*Joint Institute for Nuclear Research, RU-141980 Dubna, Russia*
[2]*Institute of Nuclear Physics, Tashkent 702132, Uzbekistan*
[3]*Institut für Theoretische Physik der Justus-Liebig-Universität, D-35392 Giessen, Germany*
(Received 30 March 2006; revised manuscript received 4 May 2006; published 14 September 2006)

The low-lying alternative parity bands in heaviest nuclei are predicted for the first time. The parity splitting and electric dipole, quadrupole, and octupole transition moments of heavy nuclei are calculated within a cluster model. The model is based on the assumption that reflection asymmetric shapes are produced by the motion of the nuclear system in the mass asymmetry coordinate.

DOI: 10.1103/PhysRevC.74.034316 PACS number(s): 21.10.Re, 21.60.Ev, 21.60.Gx, 27.90.+b

I. INTRODUCTION

Lately the low-lying collective states, α decay, and K isomers are attracting much attention in the study of the structure of transfermium nuclei [1–13]. New spectroscopic data have been obtained for the heaviest nuclei with charge numbers $Z \geqslant 96$. For instance, in inbeam experiments, the rotational bands of nuclei ^{252,254}No have been identified up to spins of 20–22 [1]. The γ transitions in the rotational yrast and nonyrast bands, weakly populated isomeric levels, and α-decay fine structure are hard to observe because of low production cross sections and large backgrounds. However, the improved sensitivity of modern setups at the ANL (Argonne), GSI (Darmstadt), JYFL (Yyväskylä), GANIL (Caen), and FLNR (Dubna) laboratories allows us to measure the α-γ or α conversion-electron coincidence [1–13].

Knowledge of the structure of very heavy elements is essential to testing and developing mean-field theories that predict nuclear properties. The spectroscopic studies of nuclei in the transfermium region may help determine the order of single-particle orbitals and the appearance of shell gaps, i.e., to shed light on the next doubly magic nucleus beyond ^{208}Pb. Such investigations give information on the moments of inertia needed to extract the values of deformation parameters [1–3] which can be compared with the predicted values [14,15]. From the study of nuclear stability versus angular momentum, one can determine the maximal angular momentum [1,10] which contributes to the complete fusion and formation of superheavies [13]. Therefore, understanding the structure and properties of the heaviest nuclei would stimulate progress in the synthesis of new superheavy nuclei.

The observation of low-lying alternative parity states in the light and heavy actinides has shown that these nuclei have reflection-asymmetric shapes or are very soft with respect to reflection-asymmetric vibrations around the equilibrium shape [16,17]. It turns out that the actinides have α-clustering behavior, which is the origin of the appearance of low-lying alternative parity states [18,19]. It is natural to assume that the transactinides may have the same properties because they are good α emitters and, therefore, the α-cluster component is presented in the wave function of the ground state. The aim of the present paper is to predict the possible low-lying alternative parity states of superheavy nuclei and to explore their main collective characteristics. We apply the cluster model developed in Refs. [18,19] for the quantitative description of such states. The main idea of the model is that the dynamics of a mirror asymmetric deformation can be treated as a collective motion of nucleons between the two clusters or as the motion in the mass asymmetry coordinate. Such collective motion simultaneously creates the deformations with even and odd multipolarities. Among different cluster configurations, only the α-cluster system $^{A}Z \rightarrow {}^{A-4}(Z-2)+{}^{4}$He gives a significant contribution to the formation of low-energy nuclear states. Within our approach, the existing experimental data on the angular momentum dependence of parity splitting and multipole transition moments ($E1$, $E2$, $E3$) of the low-lying alternating parity states in the odd and even actinides $^{220-228}$Ra, ^{223,225,227}Ac, $^{222-224,226,228-232}$Th, ^{231}Pa, $^{232-234,236,238}$U, and ^{240,242}Pu and the medium-mass nuclei ^{144,146,148}Ba, ^{151,153}Pm, ^{146,148}Ce, ^{153,155}Eu, and ^{146,148}Nd are well described [18,19]. The perfect agreement between the calculated and experimental data supplies the elegant proof of the cluster features of reflection asymmetric states. The predictive power of the suggested model seems when be quite high when exploring the rotational bands in the heaviest nuclei.

II. CLUSTER MODEL

A. Hamiltonian in mass asymmetry coordinate

Instead of the parametrization of nuclear shapes in terms of quadrupole (β_2), octupole (β_3), and higher multipole deformations, the mass (charge) asymmetry coordinate $\eta = (A_1 - A_2)/(A_1 + A_2)$ $[\eta_Z = (Z_1 - Z_2)/(Z_1 + Z_2)]$, which describes a partition of nucleons between the dinuclear system (DNS) nuclei, is used as the relevant collective variable. Here, A_1 (Z_1) and A_2 (Z_2) are the mass (charge) numbers of the heavy and light nuclei of the DNS formed by two touching nuclei or clusters. The dynamic coordinate η (η_Z) is assumed to be a continuous variable [18,19]. The wave function in η can be thought of as a superposition of the mononucleus configuration with $|\eta| = 1$ and different cluster-type configurations including the α-cluster configuration with $|\eta| = |\eta^{\alpha}| = (A - 2A_1)/A = 1 - 8/A$ ($A_1 = 4$) [18,19]. Since the potential energies of configurations with a light cluster heavier than an α particle increase rapidly with decreasing $|\eta|$, for

small nuclear excitations only the oscillations in η in the vicinity of $|\eta| = 1$ are of interest, i.e., only clusterizations up to Li have to be considered. The relative weight of each cluster component to the total wave function is determined by solving the stationary Schrödinger equation [18,19]

$$\left[-\frac{\hbar^2}{2B_\eta}\frac{d^2}{d\eta^2} + U(\eta, I, K)\right]\Psi_K(\eta, I) = E(I, K)\Psi_K(\eta, I), \tag{1}$$

where B_η and $U(\eta, I, K)$ are the inertia coefficient and potential energy of collective Hamiltonian, respectively. Here, I and K are the total spin and its projection on the symmetry axis. Since the potential energy is invariant under the inversion (the reflection) $\eta \to -\eta$, every nondegenerate eigenfunction Ψ_K of collective Hamiltonian has a definite parity. For example, the ground state is symmetric, the first excited state is antisymmetric [18,19].

The rotational states are built on the vibrational states in η. The total wave function Φ_{pIMK} describing a nucleus with definite parity p is written as

$$\Phi_{pIMK} = \left(\frac{2I+1}{16\pi^2}\right)^{1/2}\left[\Psi_K(\eta, I)D^I_{MK} + p(-1)^{I+K}\Psi_{\overline{K}}(\eta, I)D^I_{M-K}\right]. \tag{2}$$

In the case of the even-even nuclei ($K = 0$) we have a set of states with $I^p = 0^+, 1^-, 2^+, 3^-, 4^+, \ldots$; i.e., the positive and negative rotational bands are built on the lowest even and odd states in η, respectively. For odd-mass nuclei, the rotational bands are built on the intrinsic state with $K \neq 0$, and all combinations $I^p = K^\pm, (K+1)^\pm, (K+2)^\pm \ldots$ are possible, which gives rise to the parity doublet structure of the rotational band. With increasing spin, the barrier between the α-cluster DNS and its mirror image becomes higher, the penetration probability of this barrier goes to zero, and, thus, we approach almost ideal alternative parity rotational bands [18,19].

B. Mass parameter

A method of calculating of B_η is described in Ref. [20]. Since B_η is a smooth function of A, it is possible to use the same value of B_η for the nuclei under consideration. We neglect the dependence of the mass parameter on η and for the mononucleus and α- and Li-cluster configurations of all nuclei considered, we set $B_\eta = (25 \times 10^4)m_0$ fm^2, where m_0 is the nucleon mass.

The mass B_η can be estimated by relating the mass asymmetry coordinate η to the octupole deformation coordinate β_3. Such a relation between η, R_m, and β_3 was derived in [21]:

$$\beta_3 = \sqrt{\frac{7}{4\pi}}\frac{\pi}{3}\eta(1-\eta^2)\frac{R_m^3}{R_0^3}, \tag{3}$$

where R_0 is the spherical equivalent radius of the corresponding compound nucleus. If we take the value of $B_{\beta_3} \approx 200\hbar^2$ MeV^{-1} known from the literature, then we obtain $B_\eta \approx (d\beta_3/d\eta)^2 B_{\beta_3} = (9.3 \times 10^4)m_0$ fm^2, which is compatible with the value used in the calculations.

C. Potential energy

The potential $U(\eta, I, K)$ of cluster systems ($|\eta| < 1$) is taken as

$$\begin{aligned} U(\eta, I, K) &= V(R_m, \eta, I, K) - B_1(\eta) - B_2(\eta) + B, \\ V(R_m, \eta, I, K) &= V_{\rm Coul}(R_m, \eta) + V_N(R_m, \eta) \\ &\quad + V_{\rm rot}(R_m, \eta, I, K), \end{aligned} \tag{4}$$

where B_1 and B_2 are the binding energies of the clusters forming the DNS at a given η, and B is the binding energy of the mother nucleus. The experimental ground-state masses [22], if available, are used in the calculations. If not, the predictions of Ref. [15] are used. Because of the normalization by B in Eq. (2), $E(I = K, K) = 0$ for the ground state. The DNS is localized in the minimum of the pocket of the nucleus-nucleus interaction potential V at $R = R_m$ corresponding to the touching configuration. The deformations of heavy clusters, are taken from Refs. [15,23]. The polarization effects can be neglected in the very asymmetric DNS considered. One can disregard the change of the deformation of the heavy cluster under the influence of the α particle. The polarization effects are more important at the stronger Coulomb interaction. The pole-to-pole orientation of the deformed nuclei in the DNS gives the minimum of the potential energy. Since the mode responsible for the N/Z equilibrium in the DNS is quite fast, the potential energy U is minimized with respect to η_Z for each η. The nucleus-nucleus interaction potential V contains the Coulomb $V_{\rm Coul}$, nuclear interaction V_N, and centrifugal

$$V_{\rm rot} = \hbar^2[I(I+1) - K(K+1)]/(2\Im(R_m, \eta)) \tag{5}$$

potentials [18,19,24]. To calculate the nuclear and Coulomb interactions, we applied the exact double folding procedure [18,19,24]. The potential V_N is obtained with the density-dependent nucleon-nucleon forces [24,25]. The parameters of the nucleon-nucleon interaction are fixed in nuclear structure calculations [25]. For the touching configuration, the assumption on the frozen density profiles plays no role. At $R > R_m$, almost all methods of calculating the nuclear interaction lead to close results if the values and positions of the Coulomb barriers are well described with these methods. In calculations, the nuclear density distribution is approximated by the Fermi distribution with a radius parameter 1.15 fm for the transactinides region. While for ^{4}He and ^{7}Li the diffuseness parameter a of this distribution is taken as 0.48 fm, we set $a = a_0\sqrt{B_n^{(0)}/B_n}$ fm for the heavy clusters where B_n and $B_n^{(0)}$ are the neutron binding energies of the studied nucleus and of the heaviest isotope considered for the same element, respectively. For even and odd nuclei, $a_0 = 0.56$ and 0.58 fm [18,19], respectively. If this expression gives $a < 0.52$ fm for some isotopes, we set $a = 0.52$ fm. The uncertainty of the potential energy is mainly created by the uncertainty in the definition of the diffuseness of the clusters. In our calculations, we use for all nuclei the same procedure described above to define the values of a. The details of the calculations of U as well as the solution of Eq. (1) are presented in Refs. [18,19,24].

The expression (4) cannot be used to calculate the potential energy of a mononucleus ($|\eta| = 1$); instead we use

$$U(|\eta| = 1, I, K) = U(|\eta| = 1, I = K, K) + \hbar^2[I(I+1) - K(K+1)]/[2\Im_m(|\eta| = 1)]. \quad (6)$$

The value of potential energy $U(|\eta| = 1, I = K, K)$ was chosen to obtain the correct value of energy $E(I = K, K)$ of the ground state for given B_η [18,19].

The potential energy U and, correspondingly, the moment of inertia are calculated for special cluster configurations only, namely, for the mononucleus ($|\eta| = 1$) and for the two cluster configurations with the α and Li clusters as light clusters. These calculated points are used later to smoothly interpolate the potential by a polynomial. The energies of the Li and heavier cluster configurations are much larger than the binding energies of the nuclei considered. For example, the difference between the energy of the Li cluster configuration and the binding energy of the nucleus is about 15 MeV. Therefore, we restrict our investigation to configurations with light clusters not heavier than Li.

D. Moments of inertia

To calculate the potential energy for $I \neq K$, we need the moment of inertia for the mononucleus ($|\eta| = 1$) and for the two cluster configurations with ^{4}He ($\eta = \eta^\alpha$) and ^{7}Li ($\eta = \eta^{\rm Li}$) [18,19]. The moment of inertia of the cluster configurations ($|\eta| \neq 1$) is expressed as

$$\Im(R_m, \eta) = c_1 \left(\Im_1^r + \Im_2^r + m_0 \frac{A_1 A_2}{A} R_m^2 \right), \quad (7)$$

where $\Im_i^r (i = 1, 2)$ are the rigid body moments of inertia for the DNS clusters, and $c_1 = 0.85$ [18,19] for all considered nuclei. For the mononucleus ($|\eta| = 1$), the value of the moment of inertia is not known from the data because the experimental moment of inertia is a mean value between the moment of inertia of the mononucleus and those of the cluster configurations arising as a result of the oscillations in η. We assume that

$$\Im(|\eta| = 1) = c_2 \Im^r(|\eta| = 1), \quad (8)$$

where $\Im^r$ is the rigid body moment of inertia of the mononucleus with A nucleons calculated with deformation parameters from Refs. [15,23]. The free scaling parameter c_2 is fixed by the energy of one of the known lowest states of the same parity as the parity of the ground state. Since in the isotone chain, the energy of the first excited collective state weakly depends on the charge number of the nucleus, c_2 for an unknown nucleus is adopted from the closest neighboring nucleus in the isotone chain for which the energy of one of the lowest states of the same parity as the parity of the ground state is experimentally known. The chosen values of c_2 vary within narrow intervals 0.42–0.48 and 0.5–0.8 for even-even and odd nuclei, respectively. Taking c_2 from these intervals, one can hope for reasonable predictions for nuclei whose states have not yet been measured. Uncertainty in the definition of c_2 creates the uncertainty of about 30 keV in the calculations of the energies of rotational states. The value of c_2 determines an angular momentum dependence of the α-cluster spectroscopic factor and decay width [26]. So, in our calculations there is a free parameter c_2 which models the gross behavior of the states with the same parity. However, this parameter is not responsible for describing the parity splitting studied in paper.

As we mentioned above, the moment of inertia of nucleus is a mean value between the moment of inertia of the mononucleus and those of the cluster configurations. Since the relative weights of each cluster component and mononucleus to the total wave function depend on spin, the moment of inertia $\Im(I)_{\rm eff}$ of a nucleus is a function of spin as well in our approach. The moment of inertia $\Im_{\rm eff}$ increases with spin because of the transition from the structure close to mononucleus at low I to the α-cluster structure at high I. At relatively large spins, the α-cluster configuration becomes energetically more favorable than the mononucleus configuration because $\Im(|\eta| = 1) < \Im(R_m, |\eta| < 1)$. For example, the calculated energies of the positive parity levels of the ground-state rotational bands of even-even nuclei can be described with a good accuracy by the following expression [18]:

$$E(I, K = 0) = \hbar I(I+1)/[2\Im_{\rm eff}(I)],$$
$$\Im_{\rm eff}(I) = [1 - w_\alpha(I)]\Im(|\eta| = 1) + w_\alpha(I)\Im(R_m, \eta = \eta^\alpha),$$

where $w_\alpha(I) = \int_{\eta^\alpha}^{\eta^{\rm Li}} d\eta |\Psi_K(\eta, I)|^2$ and $1 - w_\alpha(I)$ are the weights of ^{4}He-cluster and mononucleus configurations, respectively. The contributions to the wave function in η of other cluster configurations are very small.

III. RESULTS OF CALCULATIONS AND DISCUSSION

A. Calculation procedure

It is convenient to substitute the coordinate η by the following coordinate

$$x = \eta - 1 \quad \text{if } \eta > 0, \qquad x = \eta + 1 \quad \text{if } \eta < 0.$$

Then the Schrödinger equation (1) can be rewritten as

$$\left[-\frac{\hbar^2}{2B_x} \frac{d^2}{dx^2} + U(x, I, K) \right] \Psi_K(x, I) = E(I, K) \Psi_K(x, I), \quad (9)$$

where $B_x = B_\eta$ is the effective mass. The smooth parametrization

$$U(x, I, K) = \sum_{k=0}^{4} a_{2k}(I, K) x^{2k} \quad (10)$$

of the potential $U(x, I, K)$ is chosen. The potential energy is symmetric with respect to $x = 0$ ($|\eta| = 1$). The parameters $a_{2k}(I)$ are determined by the calculated potential values for $x = 0$ ($|\eta| = 1$), $x = x_\alpha$ ($\eta = \pm\eta^\alpha$) and $x = x_{\rm Li}$ ($\eta = \pm\eta^{\rm Li}$). The value $a_0(I = K)$ is taken so that the ground-state energy $E(I = K, K)$ is zero after the solution of the Schrödinger equation. The calculations with other parametrizations show almost no difference in the description of parity splitting in the considered nuclei.

The solution of Eq. (9) has a well-defined parity. The lower and first excited states are the symmetric and asymmetric

functions of x, respectively. For even-even nuclei, the positive (negative) parity states are built on the lowest (first excited) state in x. For odd-mass nuclei, the two lowest states obtained by solving Eq. (9) correspond to the members of a parity doublet for given spin I. The parity of the lower member of the doublet is equal to the parity p_0 of the ground state, and the higher member of the doublet has the opposite parity $-p_0$. The quantum numbers K and p_0 of the ground state of the nucleus are taken from the experiment or from theoretical predictions [27].

B. Parity splitting

With Eq. (1), we calculate the alternative parity states of ground-state rotational bands for several isotopes of U, Pu, Cm, Cf, Fm, No, Rf, and Sg. The results of these calculations are presented in Figs. 1 and 2, and Tables I–VI. They agree well with the available experimental data [27] for nuclei ^{239}U, ^{241,242,244}Pu, ^{245,248}Cm, and ^{247}Cf (positive and negative parity states) and for ^{243}Pu, ^{243,244,246,247}Cm, $^{248-250}$Cf, ^{249,251}Fm, and ^{252,254}No [positive or negative (for odd nuclei) parity states]. One can see in the rotational bands of ^{241,242,244}Pu, ^{245,248}Cm, and ^{247}Cf an appreciable shift (parity splitting) of the negative parity states with respect to the positive parity states. A good description of the experimental data, especially of the variation of the parity splitting with A at low I and of the value of the critical angular momentum at which the parity splitting disappears, means that the dependence of the potential

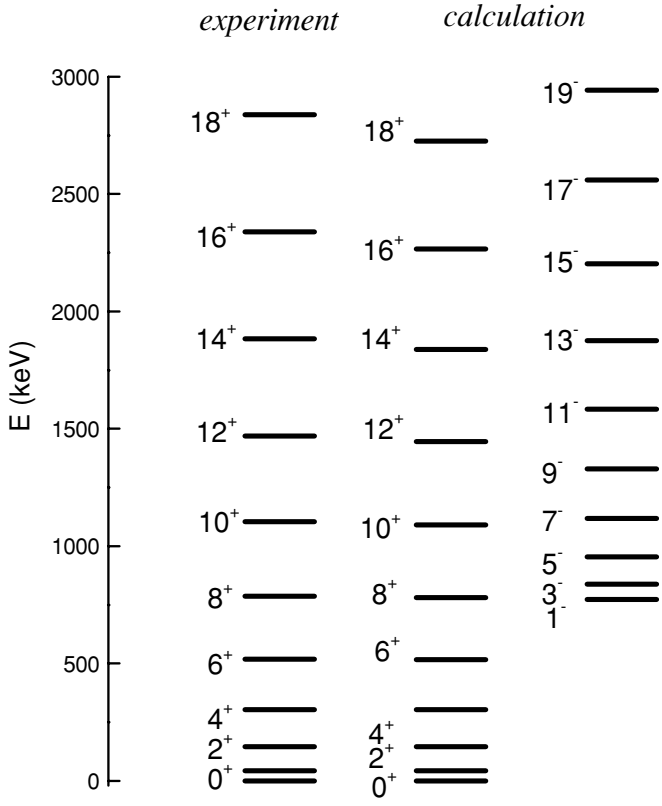

FIG. 1. Calculated level schemes in ^{254}No.

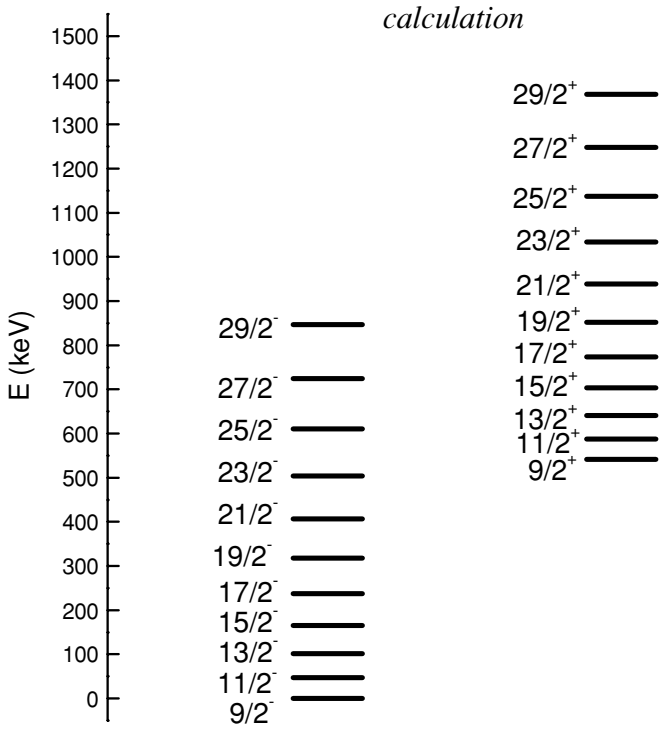

FIG. 2. Same as Fig. 1, but for ^{253}No.

energy on η and I for the nuclei of ^{241,242,244}Pu, ^{245,248}Cm, and ^{247}Cf is correctly described with our cluster model.

The alternative parity states are predicted in nuclei ^{239,240}U, ^{243}Pu, ^{243,244,246,247}Cm, $^{245,246,248-250}$Cf, $^{247-252}$Fm, $^{249-254}$No, $^{253-256}$Rf, and ^{258}Sg. In these nuclei there is also an appreciable shift of the negative parity states with respect to the positive parity states. The model parameters do not vary much from one nucleus to another. Therefore, the unknown nucleus can be predicted with high accuracy. For example, our predictions for the positive and negative parity states of ^{240}U are in good agreement with recent new experimental data [28].

One should note that the alternative parity states in the yrast rotational band of heaviest nuclei ($Z \geqslant 100$) have not yet been found in the experiments. However, there is known 3^- state of nonyrast structure at the excitation energy of 987 keV in ^{254}No [10] which is close to our predicted 3^- yrast state. Perhaps the lack of other negative parity states in the present experimental yrast rotational bands can be explained by the difficulties in detecting these states because of the small production cross sections, large background, strong competition between the channels of γ decay and emission of conversion electrons, and appreciable shift of the states with different parities. Further experimental and theoretical investigation of the predicted negative and positive parity partners is necessary.

C. Intrinsic electric multipole moments

With the wave functions obtained from Eq. (1), we calculate the electric multipole moments $Q_1 = 2D_0$, Q_2 and Q_3 defined in Refs. [18,19,21]. The effective charge for $E1$ transitions is

TABLE I. Calculated (E) and experimental ($E_{\rm exp}$) energies (in keV) of the levels of ground-state rotational band ($K^p = 0^+$) in $N = 152$ isotones. Experimental data are taken from Ref. [27].

I^p	^{248}Cm		^{250}Cf		^{252}Fm		^{254}No		^{256}Rf		^{258}Sg	
	E	$E_{\rm exp}$	E	$E_{\rm exp}$	E	$E_{\rm exp}$	E	$E_{\rm exp}$	E	$E_{\rm exp}$	E	$E_{\rm exp}$
0^+	0	0	0	0	0	0	0	0	0		0	
1^-	865	1049	823		811		773		726		661	
2^+	43	43	43	43	47	47	44	44	44		42	
3^-	930	1094	888		881		838		790		723	
4^+	143	144	143	142	155		146	145	145		140	
5^-	1046	1172	1003		1003		954		905		832	
6^+	298	298	297	296	322		304	304	303		293	
7^-	1211		1167		1177		1119		1068		987	
8^+	504	505	503	500	544		516	518	514		497	
9^-	1423		1375		1398		1330		1276		1185	
10^+	760	761	757		818		780	786	776		750	
11^-	1677	1680	1625		1661		1583		1526		1422	
12^+	1061	1061	1056		1138		1091	1104	1085		1048	
13^-	1970	1938	1912		1963		1876		1815		1695	
14^+	1404	1403	1394		1500		1445	1470	1437		1387	
15^-	2299	2238	2233		2297		2203		2136		1999	
16^+	1784	1780	1767		1899		1838	1884	1827		1762	
17^-	2658	2574	2583		2659		2560		2486		2328	
18^+	2197	2188	2175		2330		2267	2340	2251		2167	
19^-	3045	2944	2957		3044		2942		2858		2677	
20^+	2641	2622	2609		2787		2725	2839	2702		2667	
21^-	3456	3344	3353		3445				3248		3103	

TABLE II. Calculated (E) and experimental ($E_{\rm exp}$) energies (in keV) of the levels of ground-state rotational band ($K^p = 0^+$) in $N = 150$ isotones. Experimental data are taken from Ref. [9,27].

I^p	^{244}Pu		^{246}Cm		^{248}Cf		^{250}Fm		^{252}No		^{254}Rf	
	E	$E_{\rm exp}$	E	$E_{\rm exp}$	E	$E_{\rm exp}$	E	$E_{\rm exp}$	E	$E_{\rm exp}$	E	$E_{\rm exp}$
0^+	0	0	0	0	0	0	0		0	0	0	
1^-	804		797		797		782		692		596	
2^+	44	44	43	43	42	42	42		46	46	45	
3^-	870	957	862		861		845		760		660	
4^+	145	155	143	142	141	138	139		154	154	150	
5^-	989	1068	978		976		957		880		775	
6^+	303	318	298	295	294	285	290		321	321	313	
7^-	1157	1206	1144		1139		1117		1050		937	
8^+	515	535	507	500	500		492		545	545	530	
9^-	1373	1395	1356		1348		1322		1268		1143	
10^+	779	802	765		755		743		822	822	799	
11^-	1634	1628	1612		1600		1569		1589		1390	
12^+	1090	1116	1071		1057		1041		1148	1150	1115	
13^-	1936	1904	1908		1893		1855		1827		1671	
14^+	1445	1471	1421		1402		1381		1520	1526	1472	
15^-	2275	2220	2241		2221		2177		2159		1980	
16^+	1841	1864	1811		1787		1760		1930	1942	1862	
17^-	2647	2573	2606		2583		2530		2517		2384	
18^+	2273	2289	2236		2208		2174		2372	2396	2332	
19^-	3049	2958	3001		2972		2911		2894		2705	
20^+	2738	2742	2694		2660		2619		2907	2879	2731	
21^-	3475	3365	3419		3386		3315		3343		3045	

TABLE III. Calculated (E) and experimental (E_{exp}) energies (in keV) of the levels of ground-state rotational band ($K^p = 0^+$) in $N = 148$ isotones. Experimental data are taken from Ref. [27].

I^p	^{240}U		^{242}Pu		^{244}Cm		^{246}Cf		^{248}Fm		^{250}No	
	E	E_{exp}	E	E_{exp}	E	E_{exp}	E	E_{exp}	E	E_{exp}	E	E_{exp}
0^+	0		0	0	0	0	0	0	0	0	0	
1^-	838		754	781	770		768		707		592	
2^+	45		45	45	43	43	44	44	44	44	43	
3^-	907		822	832	835		834		772		654	
4^+	151		150	147	143	142	145		145		142	
5^-	1035		943	927	951		951		887		764	
6^+	314		311	306	298	296	302		302		295	
7^-	1205		1114		1115		1116		1050		920	
8^+	532		527	518	504	502	511		512		498	
9^-	1428		1331		1325		1327		1258		1117	
10^+	801		793	779	759		770		770		749	
11^-	1696		1592		1576		1580		1507		1353	
12^+	1116		1105	1084	1059		1073		1073		1043	
13^-	2003		1890		1865		1870		1791		1622	
14^+	1473		1458	1432	1398		1416		1415		1374	
15^-	2346		2223		2188		2194		2107		1919	
16^+	1868		1847	1817	1774		1796		1792		1736	
17^-	2720		2585		2540		2546		2450		2239	
18^+	2296		2269	2236	2188		2207		2200		2125	
19^-	3120		2971		2917		2922		2815		2656	
20^+	2753		2718	2686	2616		2645		2632		2596	
21^-	3544		3377		3315		3318		3196		2984	

TABLE IV. Calculated (E) and experimental (E_{exp}) energies (in keV) of the levels of ground-state rotational band ($K^p = 9/2^-$) in $N = 151$ isotones. Experimental data are taken from Ref. [27].

I^p	^{245}Pu		^{247}Cm		^{249}Cf		^{251}Fm		^{253}No		^{255}Rf	
	E	E_{exp}	E	E_{exp}	E	E_{exp}	E	E_{exp}	E	E_{exp}	E	E_{exp}
K^-	0	0	0	0	0	0	0	0	0		0	
K^+	608		572		545		555		542		552	
$(K+1)^-$	61		62	62	63	63	47	47	47		46	
$(K+1)^+$	665		630		602		601		588		597	
$(K+2)^-$	134		135	135	137	136	103		102		100	
$(K+2)^+$	732		697		670		656		641		650	
$(K+3)^-$	217	217	220	219	223	220	168		165		163	
$(K+3)^+$	810		775		748		718		703		711	
$(K+4)^-$	311		315		320	315	241		237		234	
$(K+4)^+$	897		862		836		790		774		780	
$(K+5)^-$	417		422		428	425	322		318		314	
$(K+5)^+$	995		961		934		869		852		857	
$(K+6)^-$	534		540		547		412		407		401	
$(K+6)^+$	1104		1069		1042		957		939		943	
$(K+7)^-$	661		669		678		511		504		497	
$(K+7)^+$	1222		1187		1160		1053		1034		1037	
$(K+8)^-$	800		809		820		618		610		602	
$(K+8)^+$	1350		1315		1288		1158		1137		1138	
$(K+9)^-$	949		961		973		734		724		715	
$(K+9)^+$	1488		1453		1426		1271		1248		1248	
$(K+10)^-$	1110		1123		1137		858		847		836	
$(K+10)^+$	1637		1601		1573		1392		1368		1366	

TABLE V. Calculated (E) and experimental ($E_{\rm exp}$) energies (in keV) of the levels of ground-state rotational band ($K^p = 7/2^+$) in $N = 149$ isotones. Experimental data are taken from Ref. [27].

I^p	^{243}Pu		^{245}Cm		^{247}Cf		^{249}Fm		^{251}No		^{253}Rf	
	E	$E_{\rm exp}$	E	$E_{\rm exp}$	E	$E_{\rm exp}$	E	$E_{\rm exp}$	E	$E_{\rm exp}$	E	$E_{\rm exp}$
K^+	0	0	0	0	0	0	0	0	0	0	0	
K^-	589		594	643	640	678	535		478		449	
$(K+1)^+$	58	58	55	55	55	55	58	58	61	61	59	
$(K+1)^-$	641		644	702	691	738	586		530		500	
$(K+2)^+$	128	125	122	122	123	122	128	128	134	117	132	
$(K+2)^-$	705		705	773	752		648		594		562	
$(K+3)^+$	211	207	201	197	202	201	211		222		217	
$(K+3)^-$	780		777	866	825		722		669		635	
$(K+4)^+$	307	299	292		294		307		322		315	
$(K+4)^-$	867		860		908		806		755		718	
$(K+5)^+$	416	404	396		398		415		435		426	
$(K+5)^-$	965		954		1003		901		852		812	
$(K+6)^+$	537	519	511		514		536		561		550	
$(K+6)^-$	1074		1059		1108		1008		959		917	
$(K+7)^+$	670	647	638		642		669		700		685	
$(K+7)^-$	1194		1174		1225		1124		1077		1031	
$(K+8)^+$	816	784	778		782		814		851		833	
$(K+8)^-$	1325		1300		1352		1251		1205		1155	
$(K+9)^+$	975	933	929		934		972		1014		991	
$(K+9)^-$	1467		1437		1489		1389		1342		1288	
$(K+10)^+$	1146	1092	1092		1098		1141		1188		1161	
$(K+10)^-$	1620		1584		1637		1536		1488		1430	

TABLE VI. Calculated (E) and experimental ($E_{\rm exp}$) energies (in keV) for the ground-state rotational band levels ($K^p = 5/2^+$) in $N = 147$ isotopes. Experimental data are taken from Ref. [27].

I^p	^{239}U		^{241}Pu		^{243}Cm		^{245}Cf		^{247}Fm		^{249}No	
	E	$E_{\rm exp}$	E	$E_{\rm exp}$	E	$E_{\rm exp}$	E	$E_{\rm exp}$	E	$E_{\rm exp}$	E	$E_{\rm exp}$
K^+	0	0	0	0	0	0	0	0	0		0	
K^-	592	539	569	519	490		462		433		307	
$(K+1)^+$	43	43	42	42	42	42	50	50	49		47	
$(K+1)^-$	632		608	561	527		505		475		346	
$(K+2)^+$	99	99	96	96	95	94	114		112		106	
$(K+2)^-$	683		658	615	576		560		529		396	
$(K+3)^+$	167		162	161	160		193		189		179	
$(K+3)^-$	746		719		635		628		594		456	
$(K+4)^+$	247		241	235	237		285		279		264	
$(K+4)^-$	820		791		705		707		671		527	
$(K+5)^+$	340		331		326		391		383		440	
$(K+5)^-$	905		873		785		798		759		693	
$(K+6)^+$	445		433		427		512		500		543	
$(K+6)^-$	1001		967		876		900		858		776	
$(K+7)^+$	562		547		539		645		631		657	
$(K+7)^-$	1101		1071		977		1013		968		868	
$(K+8)^+$	691		673		663		792		774		781	
$(K+8)^-$	1227		1186		1089		1137		1088		969	
$(K+9)^+$	833		810		798		951		929		913	
$(K+9)^-$	1356		1312		1211		1271		1217		1079	
$(K+10)^+$	987		960		945		1123		1096		1055	
$(K+10)^-$	1497		1448		1343		1415		1356		1198	

TABLE VII. Transitional electric dipole D_0, quadrupole Q_2, and octupole Q_3 moments for the transitions from the ground state to the states of alternating parity band.

Nucleus	D_0 (e fm) $(0^+ \to 1^-)$	Q_2 (e fm^2) $(0^+ \to 2^+)$	Q_3 (e fm^3) $(0^+ \to 3^-)$
^{240}U	0.0017	823	1292
^{242}Pu	0.0030	875	1432
^{244}Cm	0.0029	894	1464
^{246}Cf	0.0030	982	1538
^{248}Fm	0.0046	1012	1672
^{250}No	0.0092	1046	1920
^{244}Pu	0.0025	877	1385
^{246}Cm	0.0027	901	1441
^{248}Cf	0.0027	963	1497
^{250}Fm	0.0032	989	1573
^{252}No	0.0057	1019	1750
^{254}Rf	0.0100	1053	1978
^{248}Cm	0.0020	976	1380
^{250}Cf	0.0026	1045	1481
^{252}Fm	0.0030	1077	1548
^{254}No	0.0039	1109	1646
^{256}Rf	0.0050	1146	1758
^{258}Sg	0.0077	1183	1927

taken to be equal to $e_1^{\text{eff}} = e(1+\chi)$ with an average state-independent value of $E1$ polarizability coefficient $\chi = -0.7$ [29,30]. This renormalization considers a coupling of the mass-asymmetry mode to the giant dipole resonance in the DNS. In the case of the quadrupole transitions, we do not renormalize the charge $e_2^{\text{eff}} = e$. Taking into account the coupling of the mass-asymmetry mode with the higher-lying isovector and isoscalar octupole excitations [29,30], we set for octupole moments the effective charge $e^{\text{eff}}_{3,\text{proton}} = 1.2e$ for protons and $e^{\text{eff}}_{3,\text{neutron}} = 0.8e$ for neutrons. The results of our calculations are listed in Tables VII and VIII, and shown in Fig. 3. The predicted multipole moments have the common properties of nuclei exhibiting the features of reflection asymmetry. Our predicted values for Q_2 are in satisfactory agreement with those following from the theoretical predictions of Refs. [14,15]. The predicted $E1$ transitions between the yrast positive and negative parity states of transactinides are more than one order of magnitude weaker than those for the isotopes of the lighter actinides Rn, Ra and Th. This fact creates an additional difficulty in observing the alternative parity bands in the heaviest nuclei.

TABLE VIII. Transitional electric dipole D_0, quadrupole Q_2, and octupole Q_3 moments for the transitions from the ground state to the states of parity doublet band.

Nucleus	D_0 (e fm) $[K^\pm \to (K+1)^\mp]$	Q_2 (e fm^2) $[K^\pm \to (K+2)^\pm]$	Q_3 (e fm^3) $[K^\pm \to (K+3)^\mp]$
^{239}U	0.0075	826	1562
^{241}Pu	0.0088	851	1656
^{243}Cm	0.015	911	1888
^{245}Cf	0.018	939	2024
^{247}Fm	0.021	1010	2193
^{249}No	0.043	1061	2754
^{243}Pu	0.0086	883	1643
^{245}Cm	0.0085	910	1694
^{247}Cf	0.0066	969	1690
^{229}Fm	0.0126	1004	1945
^{251}No	0.0177	1036	2149
^{253}Rf	0.0207	1065	2300
^{245}Cm	0.0084	890	1621
^{247}Cf	0.011	917	1739
^{249}Fm	0.0128	983	1868
^{251}No	0.0121	1007	1908
^{253}Rf	0.0130	1037	1993
^{255}Sg	0.0125	1066	2048

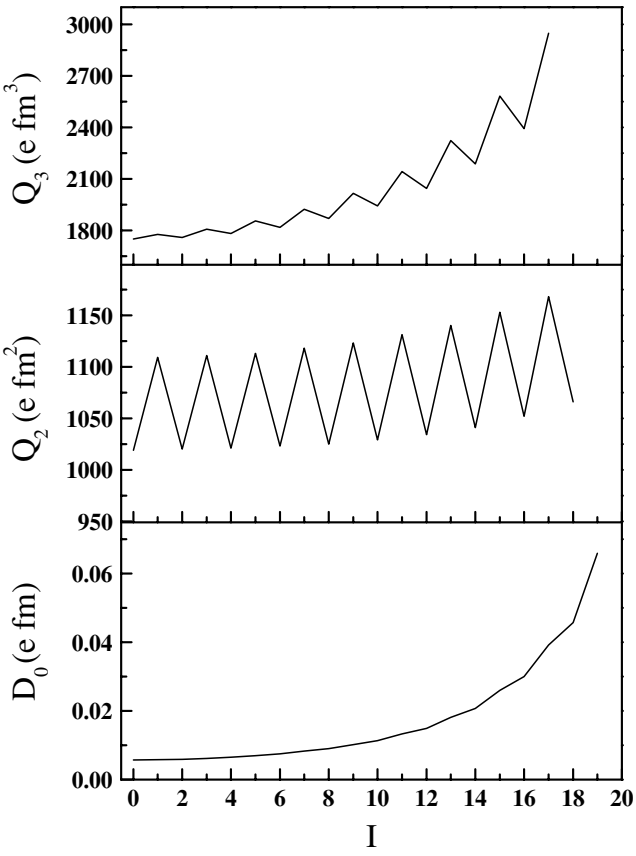

FIG. 3. Calculated spin dependences of the reduced matrix elements of the electric dipole, quadrupole, and octupole operators in ^{252}No.

The spin dependence of the reduced matrix elements of the intrinsic electric multipole operators is shown in Fig. 3 for the nucleus ^{252}No. The increase of the multipole moments with spin is similar to that observed for the reduced matrix elements in the actinides. In Fig. 3, one can see almost constant staggering of the calculated intrinsic transition quadrupole moment with the change of the parity of spin. The larger weight of the α-cluster component in the wave functions at odd I and quite large quadrupole and octupole deformations

corresponding to the α-cluster configuration explain the staggering in Q_2 and Q_3.

IV. SUMMARY

The cluster interpretation of collective low-lying alternative parity states of the nuclei with $Z \geqslant 96$ is suggested. Within the cluster approach, the α-cluster configuration gives a significant contribution to the wave function of a low-energy nuclear state. The energies of the low-lying states of the even-even and odd heaviest nuclei whose parity is opposite to the parity of the ground state are predicted. The maximal uncertainty of calculated energies of these states is about 100 keV and mainly related to the uncertainty in the calculation of the potential energy of the α-cluster configuration. The lowest energies of these states are about 600–900 keV and 300–600 keV for the even-even and odd nuclei, respectively. The observation of these states would be a crucial test of the correctness of the suggested approach. Our predictions of the spectra and intrinsic transition multipole moments will be helpful for current and future experimental works regarding the spectroscopy of superheavy nuclei.

In the future, we will treat the α-particle emission under the assumption that this cluster is formed by a collective motion of the nuclear system in η with further penetration of the α particle through the Coulomb barrier. The study of α decay widths, α fine structures and branching ratios between the α decay of a nucleus to the first rotational state and to the ground state of the daughter nucleus is important for the identification of low-lying alternative parity states.

ACKNOWLEDGMENTS

This work was supported in part by DFG (Bonn), Volkswagen-Stiftung (Hannover), and RFBR (Moscow). Support by the IN2P3-JINR (Dubna) and Polish-JINR (Dubna) Cooperation Programmes is also gratefully acknowledged. We thank professors D. Ackermann, F. P. Hessberger, A. Korichi, D. Lacroix, W. Scheid, and Ch. Thiesen for fruitful discussions and suggestions.

[1] P. Reiter *et al*., Phys. Rev. Lett. **82**, 509 (1999); **84**, 3542 (2000).
[2] M. Leino *et al*., Eur. Phys. J. A **6**, 1 (1999).
[3] F. P. Hessberger, Acta Phys. Slovaca **49**, 43 (1999); F. P. Hessberger *et al*., Eur. Phys. J. A **3**, 521 (2000); S. Hofmann *et al*., *ibid*. **10**, 5 (2001); F. P. Hessberger *et al*., *ibid*. **12**, 57 (2001).
[4] R. D. Herzberg *et al*., Phys. Rev. C **65**, 014303 (2001).
[5] P. A. Butler *et al*., Phys. Rev. Lett. **89**, 202501 (2002).
[6] M. Leino and F. P. Hessberger, Annu. Rev. Nucl. Part. Sci. **54** 175 (2004).
[7] R. D. Humphreys *et al*., Phys. Rev. C **69**, 064324 (2004).
[8] D. Ackermann, Eur. Phys. J. A **25**, 577 (2005).
[9] P. T. Greenlees *et al*., Eur. Phys. J. A **25**, 599 (2005).
[10] S. Eeckhaudt *et al*., Eur. Phys. J. A **25**, 605 (2005).
[11] P. Reiter *et al*., Phys. Rev. Lett. **95**, 032501 (2005).
[12] J. E. Bastin *et al*., Phys. Rev. C **73**, 024308 (2006).
[13] S. Hofmann and G. Münzenberg, Rev. Mod. Phys. **72**, 733 (2000).
[14] A. Sobiczewski, I. Muntian, and Z. Patyk, Phys. Rev. C **63**, 034306 (2001).
[15] P. Möller *et al*., At. Data Nucl. Data Tables **59**, 185 (1995).
[16] I. Ahmad and P. A. Butler, Annu. Rev. Nucl. Part. Sci. **43**, 71 (1993).
[17] P. A. Butler and W. Nazarewicz, Rev. Mod. Phys. **68**, 349 (1996).
[18] T. M. Shneidman, G. G. Adamian, N. V. Antonenko, R. V. Jolos, and W. Scheid, Phys. Lett. **B526**, 322 (2002); Phys. Rev. C **67**, 014313 (2003); G. G. Adamian, N. V. Antonenko, R. V. Jolos, Yu.V. Palchikov, and W. Scheid, *ibid*. **67**, 054303 (2003); G. G. Adamian *et al*., Acta Phys. Pol. B **34**, 2147 (2003).
[19] G. G. Adamian, N. V. Antonenko, R. V. Jolos, and T. M. Shneidman, Phys. Rev. C **70**, 064318 (2004); G. G. Adamian, N. V. Antonenko, R. V. Jolos, Yu. V. Palchikov, W. Scheid, and T. M. Shneidman, *ibid*. **69**, 054310 (2004).
[20] G. G. Adamian, N. V. Antonenko, and R. V. Jolos, Nucl. Phys. **A584**, 205 (1995).
[21] T. M. Shneidman, G. G. Adamian, N. V. Antonenko, S. P. Ivanova, and W. Scheid, Nucl. Phys. **A671**, 119 (2000).
[22] G. Audi, O. Bersillon, J. Blachot, and A. H. Wapstra, Nucl. Phys. **A729**, 3 (2003).
[23] S. Raman, C. W. Nestor Jr., and P. Tikkanen, At. Data Nucl. Data Tables **78**, 1 (2001).
[24] G. G. Adamian *et al*., Int. J. Mod. Phys. E **5**, 191 (1996).
[25] A. B. Migdal, *Theory of Finite Fermi Systems and Applications to Atomic Nuclei* (Wiley, New York, 1967).
[26] S. N. Kuklin *et al*., in preparation.
[27] http://www.nndc.bnl.gov/nndc/ensdf/
[28] T. Ishii *et al*., presented at the International Conference on nuclear Structure and Relative Topics, Dubna, Russia, 13–17 June, 2006.
[29] A. Bohr and B. R. Mottelson, *Nuclear Structure* (Benjamin, New York, 1975), Vol. II.
[30] I. Hamamoto, Nucl. Phys. **A557**, 515c (1992).